



UNIVERSITI PUTRA MALAYSIA

**MICROSTRUCTURES AND DIELECTRIC PROPERTIES OF Pb
(Al, V)-Oxide SYSTEMS**

WALTER CHARLES PRIMUS

FPSK(M) 2005 23

**MICROSTRUCTURES AND DIELECTRIC PROPERTIES OF
Pb(Al_xV_{1-x})O_{3±δ} SYSTEMS**

By

WALTER CHARLES PRIMUS

**Thesis Submitted to the School of Graduate Studies, Universiti Putra Malaysia,
in Fulfilment of the Requirements for the Degree of Master of Science**

April 2005



DEDICATION

I dedicate this thesis to my family especially my beloved father and mother and also to all my friends.



Abstract of thesis presented to Senate of Universiti Putra Malaysia in fulfilment of the requirements for the degree of Master of Science

**MICROSTRUCTURES AND DIELECTRIC PROPERTIES OF
Pb(Al_xV_{1-x})O_{3±δ} SYSTEMS**

By

WALTER CHARLES PRIMUS

April 2005

Chairman: Professor Abdul Halim Bin Shaari, PhD

Faculty: Science

The microstructures and electrical properties of Pb(Al_xV_{1-x})O_{3±δ} ceramic have been investigated. The samples were prepared using solid-state technique and were sintered at 800 °C, 850 °C and 900 °C. Surface morphology studies show that small grains with submicron size ~ 0.25 μm coexist with the bigger grains in micron size. As the sintering temperature increased, the grains size increase and thus become more compact. From XRD analysis, the sample structure obtained is an orthorhombic system with space group PMMA and unit cell volume is 469.595 Å³.

The dielectric constant, ε' for sample PAV 7/800, PAV 7/850 and PAV 7/900 increased as the sintering temperature increased where the values of ε' for sample sintered at 900 °C is ~ 6000 at 10⁻² Hz and ~ 90 at 1 kHz. However, the loss factor, ε'' for sample sintered at 900 °C is higher than that of other samples. The loss tangent, ε''/ε' for sample PAV 7/800, PAV 7/850 and PAV 7/900 at 1 kHz are 0.1, 0.12 and 0.16 respectively. The PAV 0.9 shows the highest ε' ~4000 at 10⁻² Hz but the ε'' for this sample is also high. This is followed by sample PAV 0.7 and PAV 0.3. Between frequencies higher than 1 kHz, the magnitudes of the ε' data dispersion (~



80) are similar for samples PAV 0.3, PAV 0.7 and PAV 0.9. At 10^{-2} Hz to 1 kHz, the dispersion of ϵ' is strongly dependent on frequency. However, the ϵ' dispersion is independent with frequency at 1 kHz to 10^5 Hz. The mechanisms that are observed from all samples are quasi dc, dipolar and barrier layer. A peak observed at 10^2 Hz is due to the ionic relaxation processes. The activation energy that is obtained from sample PAV 7/800 is 0.416. It indicates that the electrons hopping are weak. An equivalent circuit model has been proposed to represent the mechanism observed.

The conductivity, σ_{ac} is increased from 3.0×10^{-8} to 8.0×10^{-8} mho/m for sample PAV 7/800 and PAV 7/900 respectively. For other samples with different Al composition, σ_{ac} increased from 1.0×10^{-9} to 1.0×10^{-8} mho/m for sample PAV 0.3 and PAV 0.9 respectively. The σ_{ac} curve exhibits two distinct regions where the low frequency region is weakly dependent on frequency due to free charge carriers while the high frequency region is strongly dependent with frequency due to bound charge carriers in this sample. The σ_{ac} is increased from 10^{-9} to 10^{-6} mho/m for 50 °C and 200 °C respectively. The activation energy of sample PAV 7/800 and PAV 0.1 is ~ 0.65 eV and may be due to the ac conduction in terms of hopping transport of charge carrier in a narrow band of localization states as the Fermi level.

In complex impedance plots, only one semicircle is observed at low frequency and does not started from the origin due to the high frequency resistance effect. For sample PAV 7/800, the resistance obtained from the plot is 8.99×10^9 ohm/m and the value of the capacitance is 1.5×10^{-10} F. The capacitance value obtained is in the range of bulk ferroelectric mechanism. In direct current measurement, the curve obtained obeyed the Ohm's law and the activation energy increased from 0.85 eV to 1.15 eV

as the sintering temperature increases from 800 °C to 900 °C and 0.71 eV to 1.62 eV
when Al compositions increase from PAV 0.1 to PAV 0.9.

Abstrak tesis yang dikemukakan kepada Senat Universiti Putra Malaysia sebagai memenuhi keperluan untuk ijazah Master Sains

**MICROSTRUKTUR DAN SIFAT DIELEKTRIK BAGI SISTEM
 $Pb(Al_xV_{1-x})O_{3\pm\delta}$**

Oleh

WALTER CHARLES PRIMUS

April 2005

Pengurus: Professor Abdul Halim Bin Shaari, PhD

Fakulti: Sains

Mikrostruktur dan sifat elektrik bagi ceramik $Pb(Al_xV_{1-x})O_{3\pm\delta}$ telah dikaji. Sampel tersebut disediakan menggunakan teknik keadaan pepejal dan disinter pada 800 °C, 850 °C dan 900 °C. Kajian morfologi permukaan menunjukkan butiran kecil bersaiz submikron $\sim 0.25 \mu m$ wujud bersama dengan butiran besar bersaiz mikron. Peningkatan suhu sinteran menyebabkan saiz butiran bertambah besar dan seterusnya menjadi lebih padat. Daripada analisis XRD, struktur sampel ialah sistem orthorhombik dengan kumpulan ruang PMMA dan isipadu sel unit 469.595 \AA^3 .

Pemalar dielektrik, ϵ' bagi sampel PAV 7/800, PAV 7/850 dan PAV 7/900 meningkat dengan peningkatan suhu sinteran di mana nilai ϵ' bagi sampel yang disinter pada 900 °C adalah ~ 6000 pada 10^{-2} Hz dan ~ 90 pada 1 kHz. Walau bagaimanapun, faktor kehilangan, ϵ'' bagi sampel disinter pada 900 °C adalah tinggi berbanding sampel yang lain. Nilai bagi kehilangan tangen, ϵ''/ϵ' bagi sampel PAV 7/800, PAV 7/850 dan PAV 7/900 masing-masing adalah 0.1, 0.12 dan 0.16 pada 1kHz. Sampel PAV 0.9 menunjukkan nilai tertinggi $\epsilon' \sim 4000$ pada 10^{-2} Hz tetapi ϵ'' bagi sampel ini juga tinggi. Ini diikuti oleh sampel PAV 0.7 dan PAV 0.3. Pada



frikuensi tinggi daripada 1 kHz, magnitud bagi taburan data ϵ' (~ 80) adalah sama untuk sampel PAV 0.3, PAV 0.7 dan PAV 0.9. Diantara 10^2 Hz hingga 1 kHz, taburan ϵ' sangat bergantung pada frekuensi. Walau bagaimanapun, taburan ϵ' tidak bergantung pada frekuensi pada 1 kHz hingga 10^5 Hz. Mekanisme yang diperolehi daripada semua sampel ialah quasi dc, dwikutub dan lapisan halangan. Puncak yang didapati pada 10^2 Hz adalah disebabkan oleh proses relaksasi ionik. Tenaga pengaktifan yang diperolehi daripada sampel PAV 7/800 ialah 0.416 eV. Ini menunjukkan bahawa loncatan elektron adalah lemah. Model litar setara telah dicadangkan untuk mewakili mekanisme yang diperolehi.

Peningkatan konduktiviti, σ_{ac} daripada 3.0×10^{-8} kepada 8.0×10^{-8} mho/m bagi sampel masing-masing PAV 7/800 dan PAV 7/900. Bagi sampel yang lain dengan komposisi Al berbeza, peningkatan σ_{ac} dari 1.0×10^{-9} kepada 1.0×10^{-8} mho/m bagi sampel masing-masing PAV 0.3 dan PAV 0.9. Lengkuk σ_{ac} juga menunjukkan dua bahagian di mana bahagian frekuensi rendah bergantung secara lemah pada frekuensi disebabkan oleh pembawa cas bebas manakala bahagian frekuensi tinggi sangat bergantung pada frekuensi disebabkan oleh pembawa cas terikat dalam sampel ini. σ_{ac} meningkat daripada 10^{-9} kepada 10^{-6} mho/m masing-masing dan bagi 50 °C dan 200 °C. Tenaga pengaktifan bagi sampel PAV 7/800 dan PAV 0.1 ialah pada ~ 0.65 eV dan ini mungkin disebabkan oleh kekonduksian ac bagi pengangkutan loncatan oleh pembawa cas dalam jalur tenaga yang sempit bagi keadaan setempat seperti paras Fermi.

Dalam plot impedant kompleks, terdapat satu semi-bulatan diperolehi pada frekuensi rendah dan tidak bermula daripada asalan disebabkan oleh kesan rintangan frekuensi

tinggi. Bagi sampel PAV 7/800, rintangan yang diperolehi daripada plot tersebut ialah 8.99×10^9 ohm/m dan nilai kapasitan ialah 1.5×10^{-10} F. Nilai kapasitan yang dicerap ialah di dalam julat mekanisme ferroelektrik. Dalam pengukuran arus terus, data yang diperolehi mematuhi hukum Ohm dan tenaga pengaktifannya meningkat daripada 0.85 eV kepada 1.15 eV apabila suhu sinteran meningkat dari 800 °C kepada 900 °C dan 0.71 eV kepada 1.62 eV apabila komposisi Al bertambah dari PAV 0.1 kepada PAV 0.9.



ACKNOWLEDGEMENTS

First and foremost I would like to express my utmost gratitude to Prof. Dr. Abdul Halim Shaari, Assoc. Prof. Dr. Wan Mohd. Daud Wan Yusoff and Assoc. Prof. Dr. Zainal Abidin Talib for their constant monitoring, supporting, encouragement and sponsoring during the period of research. Working with them has provided me with a vast understanding on the materials science and theoretical experiences from which I will continue to draw benefit in the future.

I would like to thank to Dr. Jumiah Hassan, Dr. Iftetan, Dr. Lim Kean Pah, Dr. Abdulah Cik, Dr. Kabashi, Mrs. Ari, Mrs. Jannah, Mrs. Masriani, Mr. Somsamthat, INFOPORT staff, XRD lab officer and all my lab-mates for their tremendous assistance and support throughout this study.

My appreciation also goes to my closest friend Clifford, Jerome, Constantine, Cornelius, Syamsuar, and Tini, and also to my housemate and state-mate for their support and encouragement.

Finally, the most appreciation I would like to express to my family especially to my father, Charles Primus and my mother, Margaret Pang Sue Yin, my aunt, my uncle and my cousins for their support, encouragement and prayer.



I certify that an Examination Committee met on 14th April 2005 to conduct the final examination of Walter Charles Primus on his Master of Science thesis entitled “Microstructures and Dielectric Properties of $Pb(AI_xV_{1-x})O_{3+\delta}$ Systems” in accordance with Universiti Pertanian Malaysia (Higher Degree) Act 1980 and Universiti Pertanian Malaysia (Higher Degree) Regulations 1981. The Committee recommends that the candidate be awarded the relevant degree. Members of the Examination Committee are as follows:

SIDEK ABDUL AZIZ, PhD

Associate Professor
Faculty of Science
Universiti Putra Malaysia
(Chairman)

JUMIAH HASSAN, PhD

Faculty of Science
Universiti Putra Malaysia
(Internal Examiner)

NOORHANA YAHYA, PhD

Faculty of Science
Universiti Putra Malaysia
(Internal Examiner)

IBRAHIM ABU TALIB, PhD

Professor
Faculty of Science and Technology
Universiti Kebangsaan Malaysia
(External Examiner)



GULAM RUSUL BAHMAT ALI, PhD
Professor/Deputy Dean
School of Graduate Studies
Universiti Putra Malaysia

Date: 19 MAY 2005

This thesis submitted to the Senate of Universiti Putra Malaysia and has been accepted as fulfillment of the requirement for the degree of Master of Science. The members of the Supervisor Committee are as follows:

ABDUL HALIM SHAARI, PhD

Professor
Faculty of Science
Universiti Putra Malaysia
(Chairman)

WAN MOHD. DAUD WAN YUSOFF, PhD

Associate Professor
Faculty of Science
Universiti Putra Malaysia
(Member)

ZAINAL ABIDIN TALIB, PhD

Associate Professor
Faculty of Science
Universiti Putra Malaysia
(Member)



AINI IDERIS, PhD

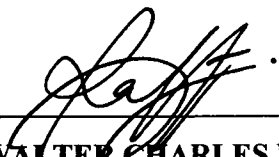
Professor/Dean
School of Graduate Studies
Universiti Putra Malaysia

Date: 09 JUN 2005



DECLARATION

I hereby declare that the thesis is based on my original work except for quotations and citations which have been duly acknowledged. I also declare that it has not been previously or concurrently submitted for any other degree at UPM or other institutions.



WALTER CHARLES PRIMUS

Date: 18 May 2005



TABLE OF CONTENTS

	Page
DEDICATION	II
ABSTRACT	III
ABSTRAK	VI
ACKNOWLEDGEMENTS	IX
APPROVAL	X
DECLARATION	XII
LIST OF TABLES	XV
LIST OF FIGURES	XVI
LIST OF PLATE	XIX
LIST OF ABBREVIATIONS/NOTATIONS/GLOSSARY OF TERMS	XX

CHAPTER

1	RESEARCH OVERVIEW	1
	1.1 Introduction	1
	1.2 Objective	2
	1.3 Brief Literature	3
2	LITERATURE REVIEW	5
	2.1 Introduction	5
	2.2 Dielectric Ceramic Materials	6
3	THEORY	10
	3.1 Dielectric Definition	10
	3.2 Dielectric Polarization Mechanisms	15
	3.3 Dielectric Relaxation Concept	18
	3.4 Immittance Spectroscopy	19
	3.5 Universal Capacitor Responses	21
	3.6 AC Conductivity	26
	3.7 Complex Plane Analysis	27
	3.8 DC Conductivity	31
4	MATERIAL, METHODOLOGY AND APPARANTUS	32
	4.1 Chemical	32
	4.2 Sample Preparation	32
	4.3 Equipment Measurement	35
	4.3.1 Thermal Analysis	35
	4.3.2 X-Ray Diffraction (XRD)	36
	4.3.3 Scanning Electron Microscope (SEM) and Electron Dispersion X-ray (EDX)	37
	4.3.4 Dielectric Spectrometer	37
	4.3.5 Direct Current Conductivity	39



4.4	Experiment Error	39
5	RESULTS AND DISCUSSION I	
	Thermal Analysis and Microstructural Properties	40
5.1	Introduction	40
5.2	Thermal Analysis For $\text{Pb}(\text{Al}_{1/2}\text{V}_{1/2})\text{O}_3$ Ceramic	40
5.3	Structural Analysis	43
5.4	Surface Morphology	46
	5.4.1 Surface morphology of different sintering temperatures	46
	5.4.2 Surface morphology after annealing in air and oxygen	48
	5.4.3 Surface morphology of different composition	56
5.5	Element Analysis	59
	5.5.1 Element analysis in different sintering temperature	59
	5.5.2 Element analysis in different composition	61
6	RESULTS AND DISCUSSION II	
	Dielectric Properties	64
6.1	Introduction	64
6.2	Frequency Dependence of Dielectric Permittivity	64
6.3	Frequency Permittivity of Annealed Samples	71
6.4	Dielectric Response With Equivalent Circuit Modeling	78
6.5	AC Conductivity in Frequency Domain	94
6.6	Complex Plane Analysis	102
6.7	DC Conductivity Measurement	113
7	CONCLUSION AND SUGGESTION	117
	REFERENCES	120
	APPENDICES	123
	BIODATA OF THE AUTHOR	138



LIST OF TABLES

Table		Page
3.1	The summary of various spectral functions and their power law exponents.	14
3.2	Capacitance values and their possible interpretation.	30
4.1	Chemicals list.	32
4.2	The first series of PAV sample's preparation.	34
4.3	The second series of PAV samples preparation.	35
5.1	The axial lengths and angles for orthorhombic system.	45
5.2	Atomic % for each element at four spectrums for sample PAV 7/800 (a), PAV 7/850 (b) and PAV 7/900 (c).	60
5.3	The atomic % for each element for sample (a) PAV 0.1, (b) PAV 0.3, (c) PAV 0.7 and (d) PAV 0.9.	63
3.9	The fitting values for sample PAV 7/800, PAV 7/850 and PAV 7/900.	80
6.2	Parameter value for fitting experimental data for sample PAV 0.1, PAV 0.3, PAV 0.7 and PAV 0.9.	83
6.3	Parameter value for fitting experimental data for sample PAV 7/800.	87
6.4	Parameter value for fitting experimental data for sample PAV 0.1.	91
6.5	Parameter value for fitting the experimental data in Figure 6.17.	93
6.6	Fitting parameter for ac conductivity of sample PAV 0.1 at four different temperatures.	100
6.7	Fitted values for the complex impedance plots for samples PAV 7/800, PAV 7/850, and PAV 7/900 at different sintering temperatures.	104
6.8	Fitted values for the complex impedance plots for sample PAV 7/850 at various temperatures.	110



LIST OF FIGURES

Figure		Page
2.1	Structure of ordered perovskite $\text{Pb}(\text{Sc}_{1/2}\text{Ta}_{1/2})\text{O}_3$.	9
3.1	Condenser in vacuum (a) and filled with dielectric materials (b) connected to a source of steady voltage.	10
3.2	The various types of interaction between the electromagnetic field and matter and the relevant relative permittivity.	15
3.3	The polarization process with no electric field and with applied electric field.	17
3.4	Dielectric relaxation spectra showed the single relaxation time.	19
3.5	The quasi dc dispersion and its circuit element.	23
3.6	The dipolar dispersion and its circuit element.	24
3.7	The barrier layer dispersion and its circuit element.	25
3.8	The general classification of all types of dielectric responses found in solids.	26
3.9	(a) Schematic representation of a typical impedance diagram. The semi-circle arc inclined at an angle $n\pi/2$. (b) Circuit element representing the impedance diagram in (a).	29
4.1	Schematic representation of the dielectric spectrometer.	38
5.1	Thermal analysis for sample PAV.	42
5.2	(a) is the XRD patterns and (b) is the peak lines for sample $\text{Pb}(\text{Al}_{1/2}\text{V}_{1/2})\text{O}_3$ at different sintering temperatures.	44
5.3	XRD pattern with indexing for sample $\text{Pb}(\text{Al}_{1/2}\text{V}_{1/2})\text{O}_3$ sintered at 850 °C.	45
6.1	Log permittivity versus log frequency for three sintering temperatures for sample PAV.	65
6.2	Log permittivity versus log frequency for different composition of sample PAV.	66
6.3	Graph of double log permittivity versus frequency for sample PAV 7/800 at different temperatures.	68



6.4	Graph of double log permittivity versus frequency for sample PAV 0.1 at different temperatures.	70
6.5	Complex dielectric permittivity versus frequency for sample PAV 7/800 annealed at 750 °C in oxygen and air.	72
6.6	Complex dielectric permittivity versus frequency for sample PAV 7/850 annealed at 750 °C and 800 °C in oxygen and air.	73
6.7	Complex dielectric permittivity versus frequency for sample PAV 7/900 annealed at 750 °C, 800 °C and 850 °C in oxygen and air.	76
6.8	Fitted graph of double log $C'(\omega)$ and $C''(\omega)$ versus frequency for sample PAV 7/800, PAV 7/850 and PAV 7/900 .	79
6.9	The circuit model represents the response mechanism polarization for samples different sintering temperature at room temperature.	80
6.10	Fitted graph of double log $C'(\omega)$ and $C''(\omega)$ versus frequency for sample PAV 0.1, PAV 0.3, PAV 0.7 and PAV 0.9 measured at room temperatures.	81
6.11	Fitted graph of double log $C'(\omega)$ and $C''(\omega)$ versus frequency for sample PAV 7/800 at different temperatures.	85
6.12	The circuit model represents the response mechanism polarization in samples PAV 7/800 at 200 °C.	87
6.13	Arrhenius plot for $\ln f_c$ versus temperature for sample PAV 7/800.	87
6.14	Fitted graph of double log $C'(\omega)$ and $C''(\omega)$ versus frequency for sample PAV 0.1 at different temperatures.	89
6.15	The circuit model represents the curve in Figure 6.14.	91
6.16	Arrhenius plot for $\ln f_c$ versus temperature for sample PAV 0.1.	92
6.17	Fitted graph of double log $C'(\omega)$ and $C''(\omega)$ versus frequency for uncoated sample PAV 7/800 at 50 °C.	92
6.18	The circuit model represents the curve in Figure 6.17.	93
6.19	Graph of log ac conductivity versus log frequency for sample PAV 7/800, PAV 7/850, and PAV 7/900.	94



6.20	Graph of log ac conductivity versus log frequency for sample PAV 0.3, PAV 0.7 and PAV 0.9.	95
6.21	(a) Graph of log ac conductivity versus log frequency in the function of temperatures for sample PAV 7/800. (b) Arrhenius plots of the ac conductivity at three different frequencies.	97
6.22	(a) Graph of log ac conductivity versus log frequency in the function of temperatures for sample PAV 0.1. (b) Arrhenius plots of the ac conductivity at 1.0 Hz.	98
6.23	Circuit element represented equation by (6.1), which is used to fit the ac conductivity curve in Figure 6.22(a).	100
6.24	Activation energy for sample PAV 0.1 obtained from ω_p in Table 6.6.	101
6.25	Complex impedance plots for sample (a) PAV 7/800, (b) PAV 7/850, and (c) PAV 7/900 at room temperature.	103
6.26	Combined Z'' and M'' plots as a function of frequency for sample (a) PAV 7/800, (b) PAV 7/850, and (c) PAV 7/900 at room temperature.	106
6.27	Circuit model representing the semi-circle in Figure 6.25(a to c).	107
6.28	Complex impedance plots for sample PAV 7/850 at various temperatures.	108
6.29	Combined Z'' and M'' plots as a function of frequency for sample PAV 7/850 at various temperature.	111
6.30	Resistance versus temperatures for sample at different sintering (a) and compositions (b).	114
6.31	Graph of Arrhenius plot for $\ln \sigma_{dc}$ versus temperatures at 5 volt for samples at different sintering temperatures (a) and Al compositions (b).	116
A.1	Conversion of X-ray signals into a voltage 'ramp' by the EDS detector.	128
A.2	Diagram of measured reflection for sample PAV 7/850.	131
A.3	Spectrum for sample PAV 7/800.	132
A.4	Spectrum for sample PAV 7/850.	134
A.5	Spectrum for sample PAV 7/900.	136



LIST OF PLATES

Plate		Page
5.1	The surface morphology of sample PAV 7/800, PAV 7/850 and PAV 7/900.	47
5.2	The surface morphology of sample PAV 7/800 was annealed at 750 °C in (a) oxygen and (b) in air.	50
5.3	The surface morphology of sample PAV 7/850 was annealed at 750 °C (a) in oxygen and (b) in air and 800 °C (c) in oxygen and (d) in air.	51
5.4	The surface morphology of sample PAV 7/900 was annealed at 750 °C (a) in oxygen and (b) in air, 800 °C (c) in oxygen and (d) in air and 900 °C (e) in oxygen and (f) in air.	53
5.5	Surface morphology for sample $\text{Pb}(\text{Al}_x\text{V}_{1-x})\text{O}_{3\pm\delta}$ in different x composition; x = 0.1, 0.3, 0.7 and 0.9 is shown in (a), (b), (c) and (d) respectively.	57
5.6	The surface morphology of sample PAV 7/800 with four different spots.	60
5.7	The surface morphology of sample PAV 0.1 with four spots were made in layered area and the grains area.	62



LIST OF SYMBOLS AND ABBREVIATIONS

ϵ	Dielectric permittivity
ϵ_{inf}	Dielectric permittivity at very high frequency
ϵ_r	Relative dielectric permittivity
$\epsilon(\omega)$	Dielectric permittivity as a function of angular frequency
μ	Micron
σ	Conductivity (mho/m)
$\sigma(\omega)$	Conductivity as a function of angular frequency
τ	Relaxation time (sec)
χ'	Real part of dielectric susceptibility
χ''	Imaginary part of dielectric susceptibility
ω	Angular frequency
ω_c	Critical angular frequency
ω_p	Peak angular frequency
Ω	Ohm
\AA	Angstrom unit
eV	Electron volt
exp	Exponential
f	Frequency
j	$=\sqrt{-1}$
k	Boltzmann constant
kHz	Kilohertz
ln	Natural logarithm



log	Logarithm
mHz	Milihertz
\propto	Proportional to
\rightarrow	Goes to
<	Smaller than
>	Bigger than
\sim	Approximately
Ac	Alternating current
B	Susceptance (mho)
C*	Complex Capacitance
C'	Real part of capacitance
C''	Imaginary part of capacitance
DC	Direct current
E	Activation energy
EDX	Electron Dispersion X-ray
G	Conductance
Hz	Hertz
I	Current
Im	Imaginary part
K	Kelvin
M	Modulus
M*	Complex modulus
M'	Real part of modulus
M''	Imaginary part of modulus
MHz	Megahertz



R	Resistance
Re	Real part
SEM	Scanning electron microscope
T	Absolute temperature (Kelvin)
TGA	Thermo Gravimetric Analysis
UPM	Universiti Putra Malaysia
V	Voltage
XRD	X-ray diffraction
Y^*	Complex admittance
Y'	Real part of admittance
Y''	Imaginary part of admittance
Z^*	Complex impedance
Z'	Real part of impedance
Z''	Imaginary part of impedance



CHAPTER 1

RESEARCH OVERVIEW

1.1 Introduction

Dielectric is a field of knowledge that belongs to physics, chemistry, biology and engineering. Dielectrics are not confined to the narrow area of insulators, but to any non-metal that interacts with electric or electromagnetic fields. Polarization and the dynamics of electric charges are at the heart of dielectrics. These are often described in terms of macroscopic properties such as permittivity, dielectric loss and also dielectric constant. Electrical engineers have characterized dielectrics macroscopically using field vectors, equivalent circuits and reliability statistics. In contrast, the physicist and chemist have pushed forward the understanding of dielectric response in terms of molecular and structural response and relaxation. Many of the fundamental problems have now been addressed and it is now possible to move from dielectric analysis to dielectric synthesis. This is of considerable interest to most areas of science and demonstrates the cross-disciplinary nature of dielectrics.

Not only the electrical property has been investigated but also its correlation on chemical and microstructure. Scanning Electron Microscope (SEM), Energy Dispersive Microanalysis (EDS) and X-ray diffraction (XRD) are used in hundreds of applications where knowledge of chemical information on the micro- or nano-



scale is important. Major users include industry, university research institutes and government facilities. Typical applications are in materials research, quality control, failure analysis, and forensic science. Industries that commonly use this technique include: semi-conductor and electronics, metals, ceramics, minerals, manufacturing, engineering, nuclear, paper, petroleum, bio-science, and the motor industry.

The development in electronic and related industries on dielectric materials has pushed researchers to synthesize new materials with good dielectric properties. From ABO_3 perovskite structure (ca. $BaTiO_3$) to the modification on the A and B sites, a new material with good electrical and mechanical properties has been found. Recent work has shown that the substitution on A site with Pb and some modification on B site produce a good result on its dielectric and mechanical properties. Many works have been reported on the effect of substitution and modification on B site. However substitution and modification with aluminium (Al^{3+}) and vanadium (V^{5+}) on B site have not been reported yet. In this work, the $Pb(Al_xV_{1-x})O_{3\pm\delta}$ ceramic systems has been studied and its electrical properties have been characterized.

1.2 Objective

The main objectives of this study is to characterize the $Pb(Al_xV_{1-x})O_{3\pm\delta}$ ceramic systems by TGA, XRD, SEM, EDX, dielectric spectrometer and dc conductivity measurement. A detail objective of this study was conducted in order to investigate: